

# Are conductance plateaus independent events in atomic point contact measurements ? A statistical approach.

*Thomas Leoni, Sabrina Homri, Nadine Candoni, Petar Vidakovic, Alain Ranguis, Hubert Klein and  
Philippe Dumas\**

CINaM - CNRS 3118, Aix-Marseille Université, Faculté de Luminy, Case 913, 13288, Marseille Cedex

\*Corresponding author : fax : +33 491 829 176, mail :dumas@cinam.univ-mrs.fr

Abstract: Room temperature conductance-elongation curves of gold atomic wires are measured using a Scanning Tunnelling Microscope Break Junction technique. Landauer's conductance plateaus are individually identified and statistically analysed. Both the probabilities to observe, and the lengths of the two last plateaus (at conductance values close to  $2e^2/h$  and  $4e^2/h$ ) are studied. All results converge to show that the occurrence of these two conductance plateaus on a conductance-elongation curve are statistically independent events.

Nanowires are now considered to be serious candidates for developing future generations of electronic devices. Decreasing the dimensions of objects has effectively revealed new physical phenomena related to electronic, optical, catalytic, thermal and other properties. The understanding of their structure, stability, and electron transport properties is of the paramount importance. At the bottom limit such a nanowire can be made of a single molecular chain.<sup>1</sup> Mastering the electrodes and understanding their properties at the molecular scale is a prerequisite for electrical characterization.

The observation of Landauer<sup>2</sup> conductance plateaus while breaking noble metals contacts is quite simple. It is at the level of an undergraduate laboratory experiment. A copper wire, a 1,5V battery, a series resistor and an oscilloscope with trace memory are enough to observe the phenomena. When breaking a metallic contact, either by hand either with the help of a relay<sup>3</sup>, the conductance trace will exhibit plateaus. These plateaus correspond to ballistic electron transport through nanometric-sized constrictions. It will however be rapidly experimented that all trials are not successful.

Thousands of repeated experiments with data acquisition capabilities are preferred to build a conductance histogram. Figure 1 shows such a histogram based on our own measurements displayed together with two examples of typical conductance-elongation curves.

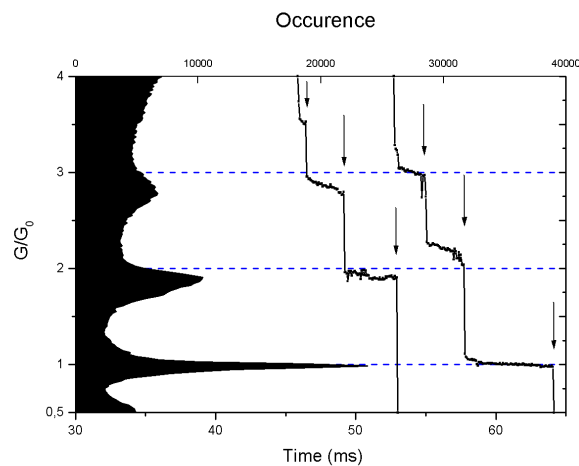


**Figure1:** Scaled conductance (vertical axis) histogram (upper horizontal axis) constructed from 9876 gold break junction curves showing the characteristic peaks close to integer multiples of the Landauer conductance quantum  $G_0=2e^2/h$ . Two conductance elongation (bottom horizontal axis, stretching rate is  $50 \text{ nm}\cdot\text{s}^{-1}$ ) curves are also shown to illustrate the appearance of the plateaus. . Room temperature data acquired with an STM-BJ at 70mV bias.

This type of histogram, widely used in the field,<sup>4,5</sup> evidences that some preferred values of conductance are observed. In the case of gold, these preferred values were shown<sup>6</sup> to be approximately integer

multiples of the Landauer conductance quantum  $G_0 = 2e^2/h$ , where  $h$  is Planck's constant and  $e$  is the electron charge.

Mechanically Controlled Break Junction (MCBJ) or Scanning Tunneling Microscopy operated in the Break Junction regime (STM-BJ) are first choice experimental methods for such conductance studies of metallic nanoconstrictions. Since the early nineties, simultaneously with an extensive theoretical work,<sup>7</sup> MCBJ and STM-BJ have been used in air<sup>5</sup>, in liquids<sup>8,9</sup> or in vacuum.<sup>4,10</sup> Direct visualization of the nanocontact has been achieved in transmission electron microscopy.<sup>11,22</sup> Conductive-AFM has allowed simultaneous measurement of the stiffness and of the conductance of the wire.<sup>12</sup> Electron-phonon interaction<sup>13</sup> and light emission<sup>14</sup> from such nanocontacts have also been reported. Since the beginning, most of the work has been devoted to metallic junctions.<sup>7</sup> Recently, a new branch is rapidly growing since the publication of the first STM-BJ measurements of single molecule conductance.<sup>15</sup>

Conductance histograms exhibiting the above mentioned characteristic preferential peaks have been obtained both at cryogenic temperatures and at room temperature.<sup>16</sup> While being powerful statistical tools, such histogram analysis considerably shrinks the data. It thus, discards and hides important information. A simple example is that, from the histogram (often plotted together with few selected conductance curves as in our own figure 1), it is impossible to know whether the conductance peak at  $G_0$  is due to  $N$  plateaus of average length  $L$  or rather due to  $N/2$  plateaus of average length  $2L$ .

To address such questions, we have undertaken STM-BJ experiments and developed the necessary software packages. In the software, for each conductance curve, the conductance plateaus, separated by abrupt changes of the conductance, are individually identified. In this paper we focus on quantities such as their average conductance and their length that are computed and statistically analyzed.

Data used in this contribution were obtained with two home-made and one commercial STM. Despite significant technical differences (vibration isolation, drift, stretching speeds,...) no significant difference was observed in the results. STM were operated at room temperature in ultra-high vacuum ( $10^{-10}$  mbar range). The commercial instrument (Omicron VT) was customized to meet the specific requirements of the experiment. The high gain in-vacuum I/V converter was short-circuited and replaced by a current limiting resistor ( $1\text{k}\Omega$ ) followed by a low-gain I/V converter ( $2 \cdot 10^5 \text{ V}\cdot\text{A}^{-1}$ ).

The samples are freshly cleaved mica sheets covered by a 100nm layer of gold with a preferential [111] orientation. Gold (99,99% purity) is deposited on heated mica sheets by electron beam evaporation under ultra high vacuum conditions. More details on gold deposition conditions and resulting properties of gold films can be found elsewhere.<sup>17</sup> After rapid transfer in air, samples are introduced in the STM chamber. Au (or Au-covered, W or Pt-Ir) metallic tips are used for the repeated nano-indentation process.

Break junction data are generated and gathered by an independent dedicated software running on a separate computer driving an input/output acquisition card. Briefly, while the STM regulation loop is maintained off, a saw tooth ramp is summed to the (constant) output of the regulation loop to bring the tip into contact prior breaking of the junction by pulling the tip away. Conductance data are simultaneously acquired at a rate of 14kHz. Typically, this sequence lasts few hundreds of milliseconds. Then the regulation loop is active again for  $\sim 1\text{s}$ . This cycle is repeated several thousands of times. While data are being acquired, the software displays each conductance-time curve and updates the above-mentioned conductance histogram (see figure1). More time-consuming processing, required for advanced statistics, is performed after acquisition.

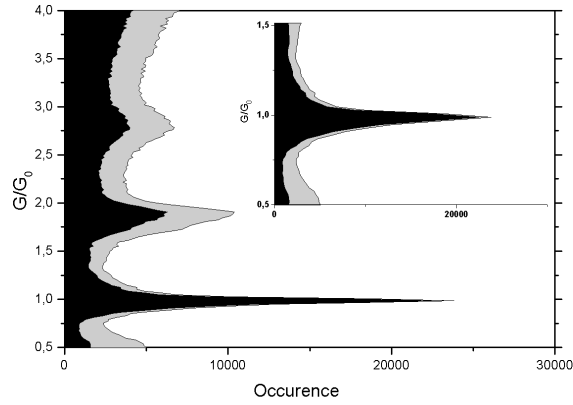
The first task of this processing is to identify the conductance plateaus. We define a plateau by a series of consecutive points (at least 3) limited by two *abrupt changes* in the conductance curve. We prefer using this criteria rather than another criteria based on the *value* of the conductance.<sup>19,25</sup>

This criteria is quite natural while it corresponds to what our eyes and brains naturally do to identify a plateau. Indeed when looking at conductance-elongation curves of figure 1 the *abrupt changes* in conductance (marked by downwards arrows) are blindingly obvious. At the contrary, it would be difficult to claim that the values of plateaus' conductance are constant and always close to integer multiple of  $2e^2/h$ . They are not<sup>18,19</sup> !

Our criteria has the second advantage of not introducing the arbitrariness of an “expected” conductance. It is not of prime importance for this study while we do not discuss here the case of molecules of unknown conductance channel transmission<sup>20</sup> but the case of gold atomic junctions, known to have a channel transmission close to one. Our criteria sets two thresholds. Abrupt changes in conductivity are associated with a conductivity change larger than  $0.15 G_0$  within one time step. This corresponds to a decay rate faster than the tunneling decay rate as observed when operating with a STM-BJ or with a MCBJ at high stretching speeds.<sup>21</sup> Plateaus shorter than three consecutive acquisition points ( $\sim 200 \mu\text{s}$  or  $10 \text{ pm}$ ) are discarded. We have checked that our results were not sensitive to variations of these thresholds.

The output of this software is that, each conductance-elongation curve could be associated with a discrete set of identified plateaus. Each of these plateaus could then be characterized in terms of average conductance, length, slope, fluctuations, etc... Finally, these data could be used for advanced statistical analysis described below.

We are now armed to analyze the results with respect to occurrence or absence of different plateaus and their eventual correlations. We recall that our experiments are made at room temperature and constant bias voltage ( $70 \text{ mV}$  is typical).



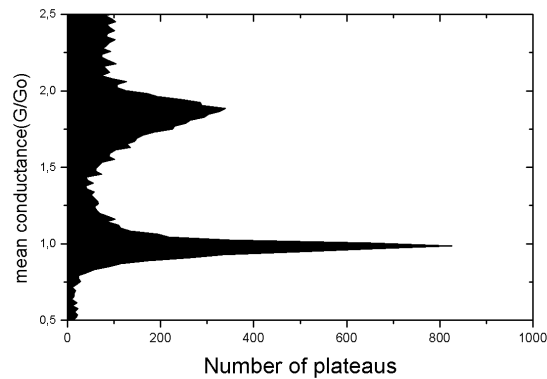
**Figure 2.** Conductance histograms of the entire set (grey) of data and of the subset (black) of the conductance-elongation curves in which a plateau around  $1.G_0$  was identified. The insert is a zoom of the  $1.G_0$  peak for which both histograms are identical. Note that histograms significantly differ around  $2.G_0$ .

Figure 2 shows two conductance histograms. In addition to the conductance histogram of a set of 9876 conductance-elongation curves, the conductance histogram of the subset of curves in which a plateau of average conductance between  $0.5G_0$  and  $1.5G_0$  is plotted. As expected, the  $1.G_0$  peaks of both histograms are superimposed. This demonstrates that our analyzing software grasps the events we are interested in. It is however noteworthy to observe that the amplitudes of the second peak (near  $2.G_0$ ) of both histograms differ significantly. This means that a noticeable number of conductance-elongation curves exhibit a plateau around  $2.G_0$  but not around  $G_0$ . Conductance-elongation curves of figure 1 are typical but were selected to show this effect. We will come back to that point later.

While our algorithm conveniently sorts the curves, we can now consider more advanced plateaus' statistics.

Instead of showing the "standard" conductance histogram, Figure 3 shows the histogram of the mean conductance value of the plateaus previously identified. With such a histogram, the length of the plateaus is disregarded. A long or a short plateau with the same average conductance will equally contribute to this histogram. It can be seen that both type of histogram display a quite similar shape. This evidences that conductance plateaus at  $IG_0$  are not longer than conductance plateaus at  $I, IG_0$ . They are only more frequently observed.

**Figure 3** Mean conductance histogram of the plateaus identified by the algorithm described in the text.



As it was stressed above, we want now to focus on the probabilities to obtain a given plateau within a large set of conductance-elongation curves. Coming back to figure 2, we can now precise that the subset of conductance curves containing a plateau around  $IG_0$  represents 61% of the complete data set containing nearly  $10^4$  curves. Let us note this probability  $P_1$ . Does this mean that we have 6 chances out of ten to obtain a plateau around  $IG_0$  when we perform a conductance curve? Not quite. Indeed, although we found a similar value (63%) for a dataset (line 9 of table 1) of more than  $10^5$  curves, we have observed fluctuations of this  $P_1$  value computed from different datasets (see table 1). These fluctuations are the result of the correlation between consecutive conductance-elongation curves. Should consecutive conductance-elongation curves be uncorrelated or statistically independent,  $P_1$  should be very close for large enough sets of data. To evidence the correlation between consecutive conductance-elongation curves, the set of 9876 curves (line 1 of table 1) was separated in two halves. From the 4938 first curves (line 3 of table 1) a  $P_1$  value of 56% is computed while from the second half (line 4 of table

1) a  $P_1$  value of 65% is computed. The net difference between these two values is very large. It corresponds to 8 times the standard deviation. In other words; we cannot assign a  $1/\sqrt{N_{\text{curves}}}$  error bar to  $P_1$ . It is why we do not discuss in this article the *absolute* value of  $P_1$  as some others groups did,<sup>22</sup> but the *conditional* probabilities which we consider more reliable.

We show now that *conditional* probabilities contain, up to now neglected in the literature as far as we are aware, valuable statistical information. Table 1 shows for different sets of data the probability  $P_1$  (respectively  $P_2$ ) to observe a plateau around  $IG_0$  (respectively around  $2.G_0$ ) together with  $P_{1\&2}$ , the probability to observe *both* plateaus on the same conductance-elongation curve.

Line	$N_{\text{curves}}$	$P_1$	$P_2$	$P_{1\&2}$	$P_1.P_2$
1	9876	61%	65%	40%	39%
2	4938	61%	64%	41%	39%
3	4938	56%	59%	35%	33%
4	4938	65%	70%	46%	46%
5	42775	54%	31%	17%	17%
6	42721	63%	44%	28%	28%
7	19356	86%	70%	61%	61%
8	1250	62%	66%	43%	41%
9	114728	63%	45%	31%	29%

**Table 1** Comparison of  $P_{1\&2}$  (column 4) and  $P_1.P_2$  (column 5). Different lines correspond to different experimental conditions (bias, STM, speed, ...) or number of conductance elongation curves ( $N_{\text{curves}}$ , column 1) used for the statistical analysis. Data of line 9 were merged regardless of the experimental conditions during acquisition. All the other figures of this article were plotted with the data corresponding to the first line of this table.

The last column contains the product  $P_1.P_2$ . The similarity between  $P_{1\&2}$  and  $P_1.P_2$  is striking for all the datasets we have investigated.  $P_{1\&2} \sim P_1.P_2$  shows that the observation of plateau 1 and the observation

of plateau 2 are independent events. When retracting the tip to break the contact, the probability to observe a plateau near  $1.G_0$  is the same, whether we have observed a plateau around  $2.G_0$  or not.

The breaking mechanism is often described as a few conductance channels sequentially broken while pulling away the contacts until the tunnel regime is reached.<sup>23</sup> In such a case, a correlation between the existence of consecutive plateaus is expected. It is not what we observe.

Another result supports this conclusion. As in our analysis the plateaus are characterized by their average conductance and lengths, the software is adapted to sort the lengths of different plateaus separately. The lengths being related in a way with the stability and life of atomic wires may serve in principle as an additional insight into complicated processes governing the breaking mechanisms. Taking advantage of the superior mechanical stability of a MCBJ design, a recent publication explores these effects for a wide range of junction stretching speeds.<sup>24</sup> Our experiments as most STM-BJ experiments correspond to stretching speeds in the high speed regime, regime for which the plateaus' length is speed independent. The histogram built for the occurrence of different lengths of the plateaus around  $1G_0$  is shown on Figure 4a. An exponential decay curve fits the data. The same procedure can be applied to the plateaus around  $2.G_0$ . The length histogram is plotted on figure 4b, together with the length histogram of the  $1.G_0$  plateaus.

It is clear that both histograms follow almost indistinguishably the same exponential decay function. Most reported room temperature length histograms exhibit a decay dependence of the probability versus the length.<sup>19,24,25</sup> We propose a simple mathematical model that accounts for the exponential decay reported here. The main aim of this simple model is to provide quantitative parameters to characterize and compare the length histograms. It does not claim to describe the physics of the breaking.

If we note  $p$ , the probability for an atomic wire to break during a time interval  $dt$ . The simplest zero-order approximation that can be made is to assume  $p$  is proportional to  $dt$  only. We thus write :

$$p = dt / \tau$$

Lets note  $P(t)$  the probability to measure a single monoatomic wire during a time  $t$  (proportional to its length).

If the wire still exists at time  $t + dt$ , this means that the wire was existing at time  $t$  and did not break during  $dt$ . Thus :

$$P(t + dt) = P(t).(1-p)$$

It is straightforward to show that :

$$P(t) = \exp(- t / \tau) / \tau$$

which corresponds to the shape of the histograms shown on figure 4.

With the breaking scenario mentioned above, system evolves from  $\sim 2.G_0$  to  $\sim 1G_0$  when one, or the other, of the monoatomic wires breaks. A statistically shorter lifetime<sup>26</sup> for the  $2.G_0$  plateau than for  $1G_0$  plateau would thus have been expected. Once more, it is not what we observe.

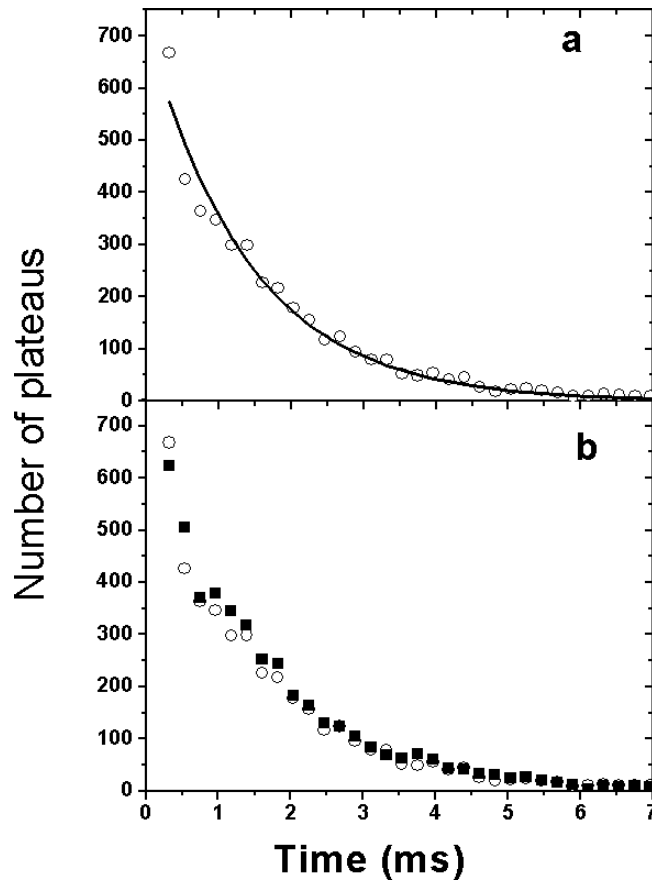


**Figure 4 :** (a) Length histogram (circle) of plateau 1. An exponential decay function (solid line) is also plotted. Its time constant is 20 ms. (b) Length histogram (squares) of plateau 2 together with length histogram (circle) of plateau 1. The decay constant is the same. The fact that the two histograms resemble is due to the coincidence that  $P_1 \sim P_2$  on this set of data.

In conclusion, conductance-elongation curves of gold nanocontacts were measured with a STM-BJ technique. By detecting the abrupt changes in the conductance, a software analysis allowed reliable identification of the plateaus. Tens of thousands of curves, acquired at room temperature, with three different STM, were statistically analyzed. Focusing on the two last plateaus, respectively around  $2.G_0$  and  $1G_0$ , we have shown that their occurrences on a conductance curve are *statistically independent events*. Length histograms also support this conclusion.

Although somewhat surprising when imagining the motion of atoms while breaking the contact, this result seems robust and was observed in all our experiments. This effect might be due to the elastic energy release when breaking the  $2.G_0$  plateau. This energy could be enough for a redistribution of all the atoms in the nanojunction. However, before proposing explanations or detailed mechanisms, it would be interesting to probe this result with independent data acquired with other apparatus especially with MCBJ's in the low speed stretching regime where breaking is dominated by the self-breaking mechanism

### **Acknowledgments**

We thank Roger Morin and Andrés Saúl for their interest and stimulating discussions.

## References

- 1 Lu, W; Lieber, C.M. *Nature Mat.* **2007**, *6*, 841.
- 2 Landauer, R. *IBM J. Res.* **1957**, *1*, 223.
- 3 Costa-Kramer, J. L.; Garcia, N.; Garciamochales, P.; Serena, P. A. *Surf. Sci.* **1995**, *342*, 1144
- 4 Krans, J. M.; Muller, C. J.; Yanson, I. K.; Govaert, T. C. M.; Hesper, R.; van Ruitenbeek, J. M. *Phys. Rev. B* **1993**, *48*, 14721.
- 5 Gai, Z.; He, Y.; Yu, H. B.; Yang, W. S. *Phys. Rev. B* **1996**, *53*, 10425.
- 6 Brandbyge, M.; Schiøtz, J.; Sørensen, M. R.; Stoltze, P.; Jacobsen, K. W.; Nørskov, J. K.; Olesen, L.; Laegsgaard, E.; Stensgaard, I.; Besenbacher, F. *Phys. Rev. B* **1995**, *52*, 8499.
- 7 Agrait, N.; Yeyati, A. L.; van Ruitenbeek, J. M. *Phys. Rep* **2003**, *377*, 81.
- 8 Diaz, M.; Costa-Kramer, J. L.; Escobar, A. L.; Leon, N.; Correia, A. *Nanotechnology* **2002**, *13*, 43.
- 9 Huang, Z.; Chen, F.; Bennett, P.A.; Tao, N.J. *J.AM.Chem.Soc.* **2007**, *129*, 13225
- 10 Agrait, N.; Rodrigo, J. G.; Vieira, S. *Phys. Rev. B* **1993**, *47*, 12345
- 11 Ohnishi, H.; Kondo, Y.; Takayanagi, K. *Nature* **1998**, *395*, 780.
- 12 Rubio-Bollinger, G.; Bahn, S. R.; Agrait, N.; Jacobsen, K. W.; Vieira, S. *Phys. Rev. Lett* **2001**, *87*, 6101
- 13 Agrait, N.; Untiedt, C.; Rubio-Bollinger, G.; Vieira, S. *Chem. Phys* **2002**, *281*, 231.
- 14 Downes, A.; Dumas, P.; Welland, M. E. *Appl. Phys. Lett.* **2002**, *81*, 1252.
- 15 Xu, B. Q.; Tao, N. J. *J. Science* **2003**, *301*, 1221.

- 16 Sirvent, C.; Rodrigo, J. G.; Agrait, N.; Vieira, S. *Physica B* **1996**, 218,238.
- 17 Klein, H.; Blanc, W.; Pierrisnard, R.; Fauquet, C.; Dumas, P. *Eur. Phys. J. B* **2000**, 14,371.
- 18 Smit, R. H. M.; Untiedt, C.; Rubio-Bollinger, G.; Segers, R. C.; van Ruitenbeek, J. M. *Phys. Rev. Lett.* **2003**, 91,6805.
- 19 Kiguchi, M.; Konishi, T.; Murakoshi, K. *Phys. Rev. B* **2006**, 73,125406.
- 20 Jang, S. Y.; Reddy, P.; Majumdar, A.; Segalman, R. A. *Nano Lett.* **2006**, 6, 2362.
- 21 Martin,C.A.;Ding,D.;van de Zant,H.S.J.;van Ruitenbeek,J.M. **2008**, ArXiv:0802.0629v2.
- 22 Rodrigues, V.; Fuhrer, T.; Ugarte, D. *Phys. Rev. Lett.* **2000**, 85, 4124.
- 23 Dreher, M.; Pauly, F.; Heurich, J.; Cuevas, J. C.; Scheer, E.; Nielaba, P. *Phys. Rev. B* **2005**, 72,5435.
- 24 Tsutsui, M.; Shoji, K.; Taniguchi, M.; Kawai, T. *Nano Lett.* **2008**, 8, 345.
- 25 Itakura, K.; Yuki, K.; Kurokawa, S.; Yasuda, H.; Sakai, A. *Phys. Rev. B* **1999**, 60, 11163.
- 26 Although the horizontal axis was kept in milliseconds to stick with raw experimental data, in this stretching speed range, the plateaus' lifetime, is indeed a plateaus' length. We have checked that doubling the elongation rate resulted in dividing the time constant by a factor of two.